Journal of Achievements in Materials and Manufacturing Engineering
VOLUME 45
ISSUE 1
March
2011

Microstructure and corrosion resistance of CrAlSiN, CrAlSiN+DLC, and CrN coatings

K. Lukaszkowicz*, W. Kwaśny, J. Szewczenko
Institute of Engineering Materials and Biomaterials, Silesian University of Technology, ul. Konarskiego 18a, 44-100 Gliwice, Poland
* Corresponding author: E-mail address: krzysztof.lukaszkowicz@polsl.pl

Received 02.01.2011; published in revised form 01.03.2011

Properties

ABSTRACT

Purpose: The main aim of the research was the investigation of microstructure and corrosion resistance of the nanostructured CrAlSiN, CrAlSiN+DLC, CrN coatings deposited by cathodic arc evaporation method onto hot work tool steel substrate.
Design/methodology/approach: Observations of surface and microstructure of the deposited coatings were carried out on cross sections in the SUPRA 35 scanning electron microscope. Diffraction and thin film microstructure were tested with the use of the JEOL JEM 3010UHR transmission electron microscope. X-ray study for the analyzed coatings was carried out using X´Pert PRO system. A phase identification of the investigated coatings was carried out in Bragg-Brentano geometry (XRD), and in grazing incidence geometry (GIXRD). Investigation of the electrochemical corrosion behaviour of the samples done in a PGP 201 Potentiostat/Galvanostat, using a conventional three-electrode cell. To simulate the aggressive media, 1-M HCl solution was used under aerated conditions and room temperature.
Findings: It was found that the microstructure of the PVD coatings consisted of fine nanocrystallites, of an average size of 8 nm -13 nm, depending on the coating type. The morphology of the coatings fracture is characteristic of a dense microstructure. Basing on the GIXRD pattern of the investigated coatings, only fcc phases was encountered. The tests carried out with the use of a GDOS technique indicate the occurrence of a transition zone between the substrate material and the coating. Deposition of the PVD coatings increases the hardness of the tool steel surface up to 22-40 GPa. The CrN coated sample showed the best corrosion resistance.
Practical implications: In order to evaluate with more detail the possibility of applying these nanocomposite coatings for protection of tool steels, further investigations should be undertaken in order to determine the thermal fatigue resistance of the coatings. The very good mechanical properties of the nanocomposite coatings make them potentially suitable for industrial applications.
Originality/value: The results of the investigation provide useful information on microstructure and protective properties of the nanocomposite coatings on hot work tool steels.
Keywords: Thin & thick coatings; Nanostructures coatings; Microstructure; Corrosion

Reference to this paper should be given in the following way:
K. Lukaszkowicz, W. Kwaśny, J. Szewczenko, Microstructure and corrosion resistance of CrAlSiN, CrAlSiN+DLC, and CrN coatings, Journal of Achievements in Materials and Manufacturing Engineering 45/1 (2011) 23-29.

1. Introduction

Nanostructured and, in particular nanocomposite coatings deposited by physical vapour deposition or chemical vapour deposition are recognised as one of very interesting premium technologies for protection and modification of products surface, for the reason of the existing possibility to synthesize materials with unique physical and chemical properties, e.g. extremely high indentation hardness (40-80 GPa) [1-3], good corrosion resistance [4, 5], excellent resistance to a high temperature oxidization [6, 7], as well as a high resistance to abrasion and erosion [8-10].

In conventional bulk materials, refining grain size is one of the possibilities for hardness increase. The same is true for nanocomposite films or coatings. With decreasing in grain size, the multiplication and mobility of dislocations are hindered, and the hardness of materials increase according to the Hall-Petch relationship. This effect is especially expedient for grain size down to tens of nanometers. However, due to instability of these defects, there are no dislocations inside the grains for the grain size smaller than 10 nm. Simultaneously, due to increasing fraction of atoms in the grain boundaries, another mechanism is responsible for the hardness of the nanocomposite coatings, i.e., the grain boundary sliding and one observes an "inverse" Hall-Petch dependence of the hardness on the grain size (Fig. 1) [11]. In order to obtain hard nanocomposite coatings particular conditions have to be fulfilled.

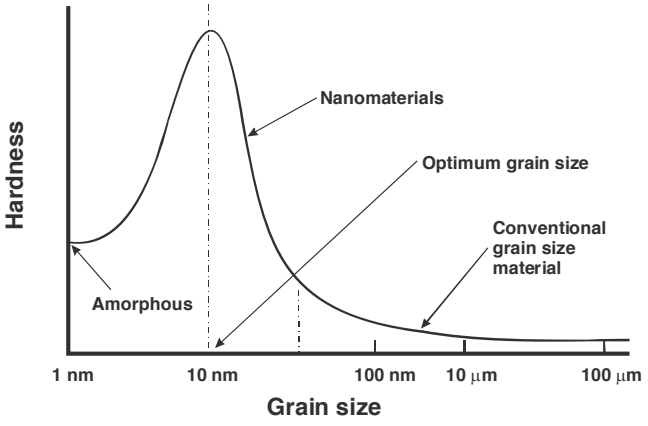

Fig. 1. Schematic illustration of materials hardness versus size of grains [11]

Multiple information connected with structure of coatings deposited by PVD technique is particularly useful for further improvement of the coating deposition process [12-14]. The structure of the PVD deposited coating is influenced by numerous parameters. On the other hand one can use a great number of research techniques to characterize composition and structure of coatings. There are, among others, the X-ray diffraction (XRD) for examination of phase composition, transmission electron microscope (TEM) for nanostructure examination and local phase identification in nanoareas, as well as scanning electron microscopy (SEM) for thorough investigations of surface and fractures morphology.

PVD hard coatings are, in general, well resistant to electrochemical corrosion. Nevertheless, a great part of PVD deposited is characteristic of a high defect density, as e.g., pores and voids between neighbouring columns enabling penetration of the aggressive agents through the coating to the substrate [15].

The purpose of this paper is to examine the microstructure and corrosion resistance of CrAlSiN, CrAlSiN+DLC and CrN coatings deposited by cathodic arc evaporation method on the X40CrMoV5-1 hot work tool steel substrate.

2. Investigation methodology

The tests were made on X40CrMoV5-1 hot work tool steel substrates with CrAlSiN, CrAlSiN+DLC and CrN hard coatings deposited by arc PVD.

Coatings` deposition was carried on in an Ar and N_2 atmosphere. Cathodes from pure metallic (Cr) or anAlSi (88:12 wt. %) alloy were used for coatings deposition. The base pressure in the vacuum chamber was 5×10^{-6} mbar. To improve coatings adhesion, a transition metal interlayer (Cr) was deposited. In case of CrAlSiN+DLC coating a DLC topcoat was deposited using acetylene (C_2H_2) as the precursor. The DLC coating produced by a PACVD process and the relevant deposition conditions are summarized in Table 1.

Observations of surface and fracture morphology of the deposited coatings were carried out using a SUPRA 35 scanning electron microscope at 4 kV energy of primary electrons and a secondary electrons imaging.

SAED electron diffraction and microstructure of thin foil cross sections were investigated with use of a JEOL JEM 3010UHR transmission electron microscope, at 300 kV bias voltage. Thin foils were prepared by mechanical grinding and further ion polishing with use of a Gatan equipment.

X-ray studies for the analyzed coatings were carried out using X´Pert PRO system made by Panalytical Company using filter radiation of a cobalt anode lamp. A phase identification of the investigated coatings was carried out in Bragg-Brentano geometry (XRD) using a Xcelerator strip detector, and a grazing incidence geometry (GIXRD) of primary beam using a collimator of parallel beam before a proportional X-ray counter.

The X-ray line broadening technique was used to determine the average crystallite size of the coatings using a Scherrer formula with Si as an internal standard:

$$d = \frac{K \cdot \lambda}{\beta \cdot \cos(\theta)} \tag{1}$$

where: d – the crystaliite size, λ is the wavelength of the X-ray radiation , K – usually taken as 0.899, β – full width at half-maximum of the (111) XRD peak (in radians), θ – the Bragg angle (in radians, as well).

The in-depth analysis of chemical composition of the deposited coatings and the substrate was carried out using a glow discharge optical spectrometer GDOS-750 QDP from Leco Instruments at the following working conditions of the spectrometer Grimm lamp:

- inner lamp diameter – 4 mm;
- lamp voltage and current – 700 V/20 mA, respectively;
- working pressure – 100 Pa.

Table 1.
Deposition parameters of the coatings

Coating	Substrate bias voltage [V]	Arc current source [A]	Pressure [Pa]	Temperature [°C]
DLC	-150	-	2.0	220
CrAlSiN	-40	Cr - 70 AlSi - 120	4.5	450
CrN	-50	Cr - 125	4.0	450

Investigation of the electrochemical corrosion behaviour of the samples were carried out in a PGP 201 Potentiostat/ Galvanostat, using a conventional three-electrode cell consisting of a saturated calomel reference electrode (SCE), a platinum counter electrode and the studied specimens as the working electrode. To simulate the aggressive media, 1M water solution of HCl was used under aerated conditions and room temperature. The aqueous corrosion behaviour of the coatings was studied first by measuring the open circuit potential (OCP) for 1 h. Subsequently, a potentiodynamic polarization curve has been recorded. The curve started at a potential of ~100 mV below the corrosion potential and ended at +1200 mV or a threshold intensity level set at 100 mA/cm^2. Once this level was reached, the reverse cycle was started. The scan rate was 15 mV/min. The corrosion current density and the corrosion potential were obtained according to a Tafel analysis of the potentiodynamic polarization curves.

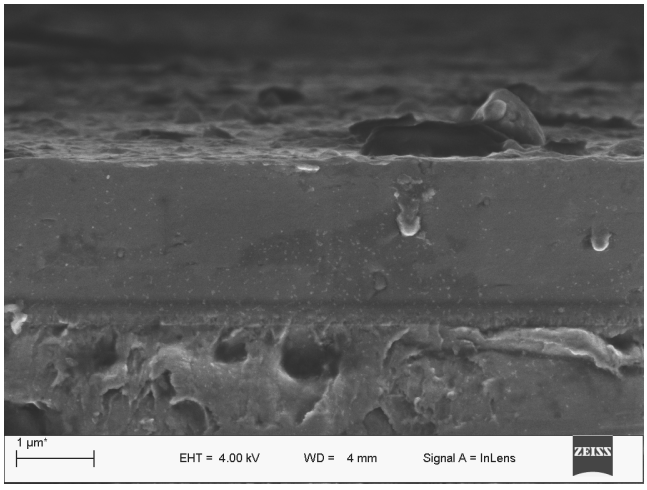

Fig. 2. Fracture of the CrAlSiN coating on the X40CrMoV5-1 hot work tool steel substrate

3. Discussion of results

The coatings have a dense and compact structure, without any visible delaminations or defects (Figs. 2-4). A thin, well determined interlayer between the coating and the substrate is well visible on the fractured cross-sections of the coated samples. The morphology of the coatings' surface is characteristic of microdroplets (Fig. 4), which are a well-known drawback of the cathodic arc evaporation. Examinations of the chemical composition of these droplets demonstrated that they developed from pure metals. This leads to the conclusion that they were ejected from boiling liquid metal in the cathode spots on the target`s surface and solidified on the substrate surface. The size of these particles changes from several tenths of 1 µm to about 4 µm.

Transmission electron microscopy (TEM) examination of the coatings showed that they consisted of fine crystallites (Fig. 5). It was deduced from TEM observations in the bright and dark fields as well as from the SAED electron diffraction, that an average size of crystallites in the CrN coating was about 8-10 nm. In case of the CrAlSiN coating the average size the of crystallites was greater.

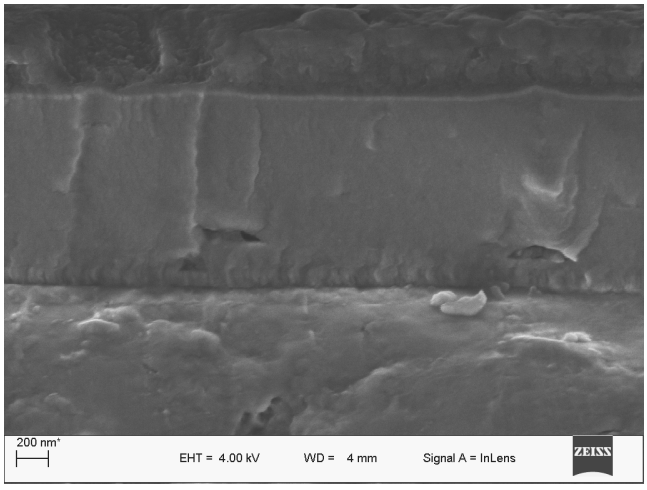

Fig. 3. Fracture of the CrAlSiN+DLC coating on the X40CrMoV5-1 hot work tool steel substrate

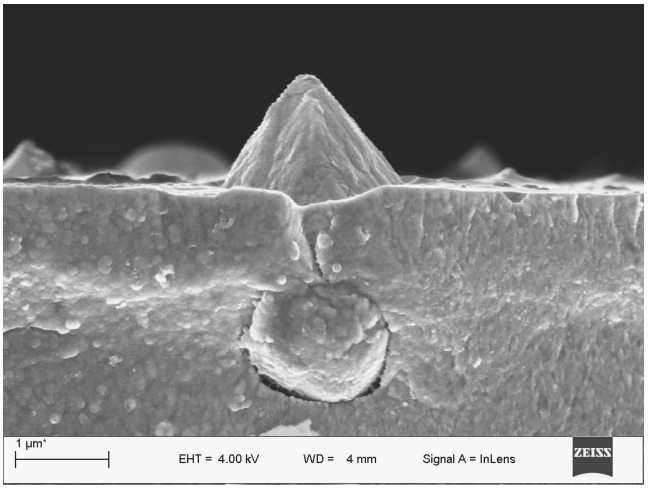

Fig. 4. Fracture of the CrN coating on the X40CrMoV5-1 hot work tool steel substrate

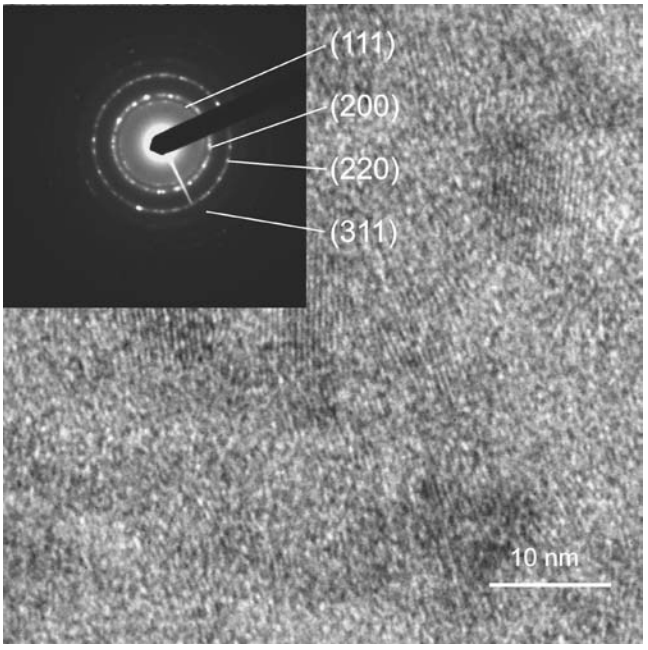

Fig. 5. TEM bright-field image and SAED electron diffraction pattern of CrAlSiN coating

The applied method of the X-ray qualitative phase analysis carried out in Bragg-Brentano geometry confirms occurrence of appropriate phases in the investigated substrate and coatings. Some of identified peaks in the analysed X-ray diffraction patterns are moved towards lower or higher angles of diffraction and their intensities differ from values given in the ICDD files for the relevant standard phases, what may indicate on occurrence of texture as well as of compressive or tensile, internal stresses in the investigated coatings. For the peaks overlapping those of the material substrate and the coating, as well as due to their low intensities, making the analysis of obtained results more difficult, an additional technique of the X-ray diffraction analysis was applied, namely a grazing incidence geometry (GIXRD). GIXRD patterns of selected coatings are presented in Figs. 6-7. Basing on the GIXRD pattern of the CrAlSiN (Fig. 6), only fcc phases were encountered in the coatings. The hexagonal AlN of wurtzite type was not discovered in the examined coatings, which could have been due to a rather small amount of aluminium in the coatings. For the CrN coating three peaks (111), (200), and (220) are shown in Fig. 7, corresponding to interplanar spacing's of 2.39, 2.07 and 1.46 Å respectively, are characteristic of the CrN cubic phase.

Based on the results obtained using the Scherer method, the average size of crystallites in the examined coatings was determined. The results are given in Table 2.

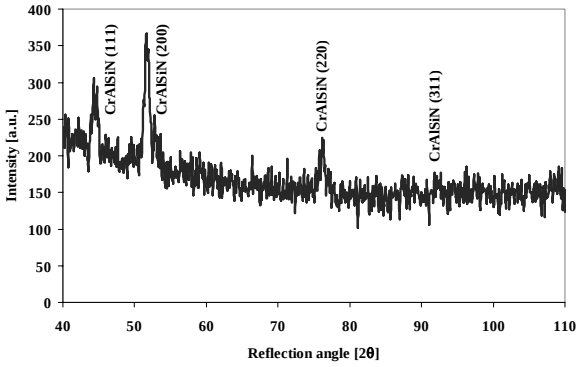

Fig. 6. GIXRD spectra of the CrAlSiN coating at an incidence angle α=3°

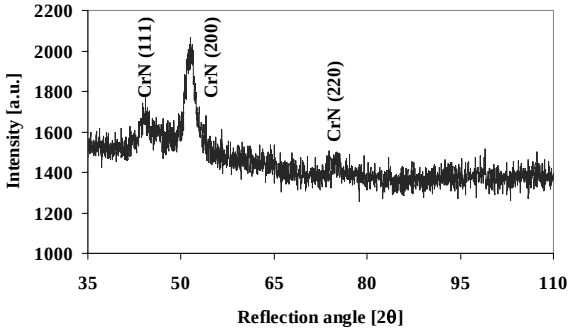

Fig. 7. GIXRD spectra of the CrN coating at an incidence angle α=1°

Texture analysis for CrAlSiN coating was carried out by a Schulz reflexion method. Regular concentric distribution of intensities in the pole figures is characteristic of an axial texture of the arc PVD deposited coating. Areas of intensity increase on recorded figures correspond to fibres presence <311>. Texture image of CrAlSiN coating presented in the form of experimental pole figures determined as CPF (Fig. 8), and complete pole figures calculated from FRO determined as RPF (Fig. 9).

Table 2.
Basic characteristics of the coatings under investigation

Coating	Thickness [μm]	Microhardness [GPa]	Crystallite size [nm]
CrAlSiN	2.1	40	13
CrAlSiN+ +DLC	1.3	40 5	11
CrN	3.2	22	8

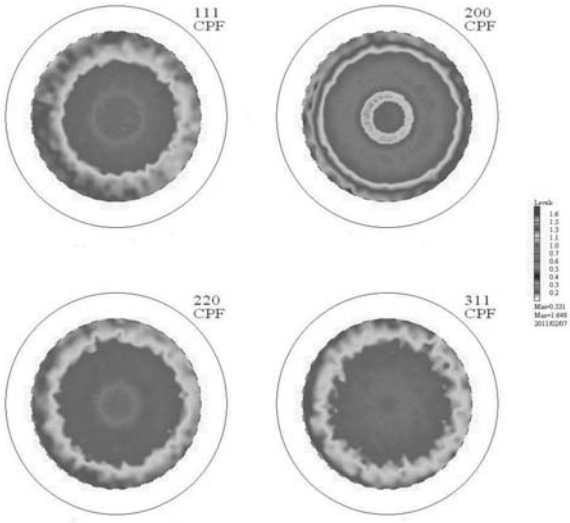

Fig. 8. Experimental (111), (200), (220), and (311) pole figure for CrAlSiN coatings deposited on the X40CrMoV5-1 hot work tool steel substrate

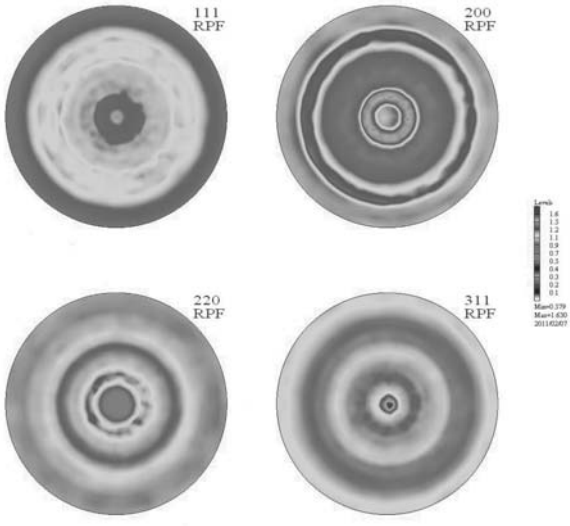

Fig. 9. (111), (200), (220), and (311) pole figures for CrAlSiN coating deposited on the X40CrMoV5-1 hot work tool steel substrate after calculation in FRO space

Calculations of volume fractions for texture components were carried out using integration of those components in FRO space subjected to transformation. In calculations of volume fractions, in identified texture components, angle broadening is taken into account ($\Delta\Phi$, $\Delta\phi_1$, $\Delta\phi_2$), which is situated in the range of 10-15º. In case of CrAlSiN coating deposited by arc PVD process volume fraction of the distinguished component <311> is approx. 15%.

In case of CrN coating, for the sake of overlapping reflexes of substrate and coating material, the texture analysis was not succeeded for the applied symmetrical Bragg-Brentano geometry of pole figures measurement.

Changes of coating component concentration and substrate material made in GDOS were presented in Figs. 10-11. The tests carried out with the use of GDOS indicate the occurrence of a transition zone between the substrate material and the coating, which results in the improved adhesion between the coatings and the substrate. In the transition zone between the coatings and the substrate, the concentration of the elements of the substrate increases with simultaneous rapid decrease in concentration of elements contained in the coatings. The existence of the transition zone should be connected with diffusion and high-energy ion action that caused mixing of the elements in the interface zone. Such results, however, cannot be interpreted explicitly, due to the non-homogeneous evaporation of the material from the sample surface. In case of the investigated coatings can clearly notice the thin chromium interlayer ,whose task is to increase the adhesion of the main coating to the substrate.

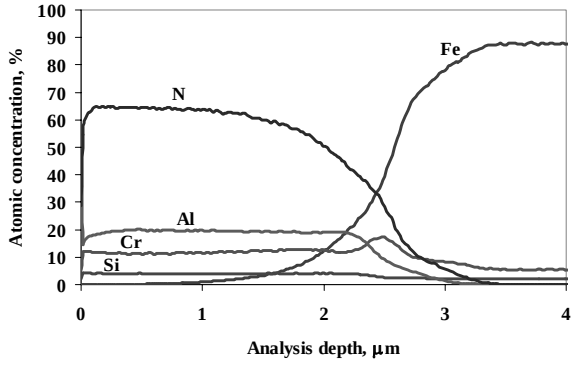

Fig. 10. GDOS concentration profiles for CrAlSiN coating on the X40CrMoV5-1 hot work tool steel substrate

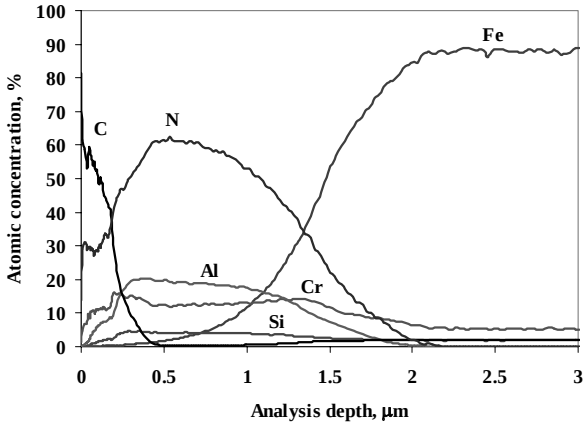

Fig. 11. GDOS concentration profiles for CrAlSiN+DLC coating on the X40CrMoV5-1 hot work tool steel substrate

The electrochemical characteristic were estimated from the potentiodynamic curves as well as from the open circuit potential measurement in 1 M water solution of HCl. The potentiodynamic polarization curves are given in Figs. 12-14. It was found, that the CrN and CrAlSiN coatings deposited by arc PVD can effectively protect the hot work tool steel X40CrMoV5-1 against the electrochemical corrosion. The lowest corrosion current density was obtained for the CrN coating, whereas for the CrAlSiN+DLC coating is significantly higher.

The results of the investigations of the open circuit potential E_{OCP} confirm the better corrosion resistance of the investigated coatings (Figs. 15-17). The relatively high initial potential value for some coatings is plausibly due to a longer time necessary for ions from the electrolyte to reach the substrate of the specimens by a slower diffusion through small surface defects.

The hardness of the X40CrMoV5-1 steel substrate without coating is 630 HV (56 HRC). After deposition of the PVD coatings it increase to a value from an interval 22-40 GPa (Table 2). The highest hardness value was obtained for the CrAlSiN coating.

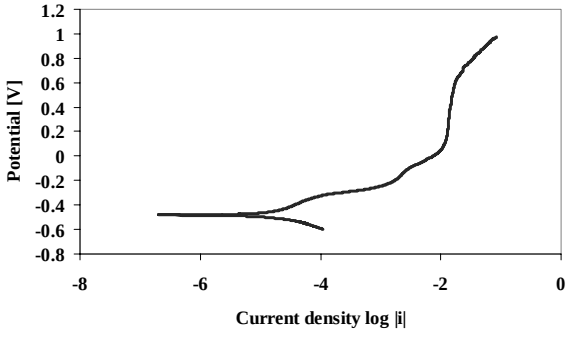

Fig. 12. Potentiodynamic polarization curves of the CrAlSiN coatings in 1 M water solution of HCl

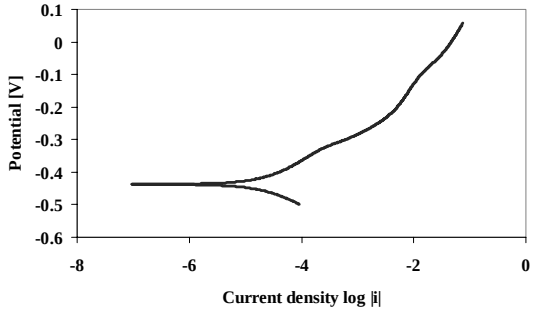

Fig. 13. Potentiodynamic polarization curves of the CrAlSiN+DLC coatings in 1 M water solution of HCl

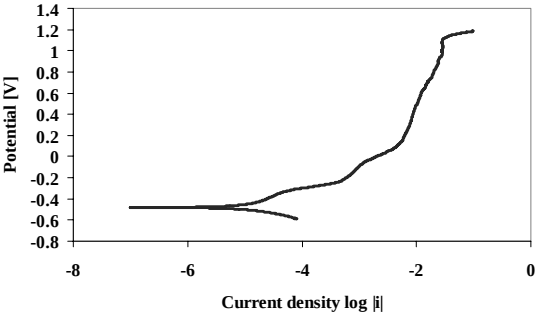

Fig. 14. Potentiodynamic polarization curves of the CrN coatings in 1 M water solution of HCl

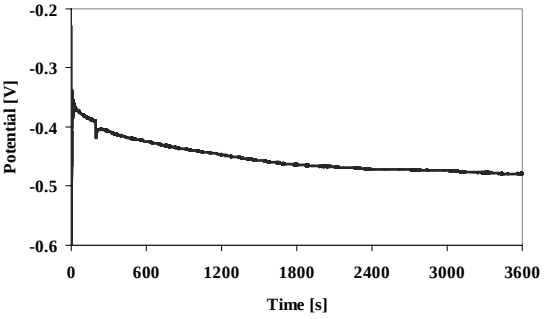

Fig. 15. Open circuit potential curve for the CrAlSiN coating in 1 M water solution of HCl

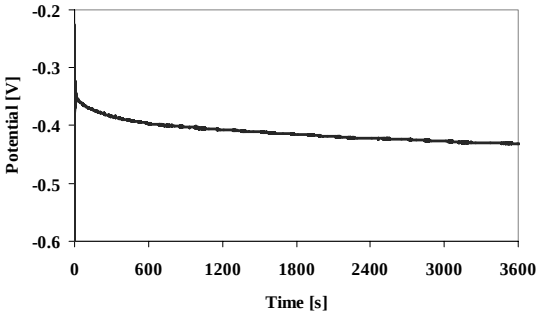

Fig. 16. Open circuit potential curve for the CrAlSiN+DLC coating in 1 M water solution of HCl

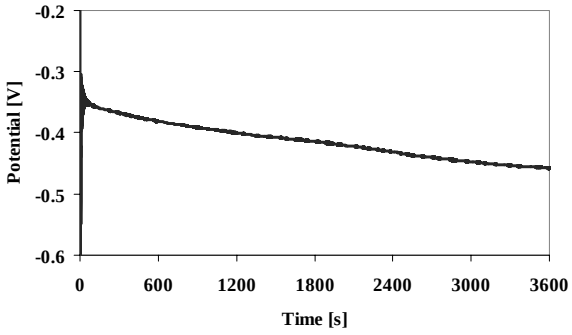

Fig. 17. Open circuit potential curve of the CrN coating in 1 M water solution of HCl

4. Summary

The CrAlSiN, CrAlSiN+DLC, and CrN coatings were deposited successfully on X40CrMoV5-1 hot work tool steel substrate. The compact microstructure of the coatings without any visible delamination was observed in the scanning electron microscope. Based on the transmission electron microscope investigations of the coatings, it was found that the coatings are nanocrystalline with the crystallites` size of 8-13 nm.

As a result of the potentiodynamic polarization curve investigations, the corrosion currents and corrosion potential were determined. The CrN coating showed the best corrosion resistance in 1 M water solution of HCl from all the investigated coatings.

Acknowledgements

Research was financed in a part within the framework of the Polish State Committee for Scientific Research Project No N N507 550738 headed by Krzysztof Lukaszkowicz, Ph.D., Eng.

References

[1] S. Veprek, M.G.J. Veprek-Heijman, The formation and role of interfaces in superhard nc-Me_nN/a-Si_3N_4 nanocomposites, Surface and Coatings Technology 201/13 (2007) 6064-6070.

[2] S. Veprek, A. Niederhofer, K. Moto, T. Bolom, H.D. Mannling, P. Nesladek, G. Dollinger, A. Bergmaier, Composition, nanostructure and origin of the ultrahardness in nc-TiN/a-Si_3N_4/a- and nc-$TiSi_2$ nanocomposites with H_v=80 to ≥105 GPa, Surface and Coatings Technology 133-134 (2000) 152-159.

[3] C.W. Zou, H.J. Wang, M. Li, Y.F. Yu, C.S. Liu, L.P. Guo, D.J. Fu, Characterization and properties of TiN-containing amorphous Ti-Si-N nanocomposite coatings prepared by arc assisted middle frequency magnetron sputtering, Vacuum 84/6 (2010) 817-822.

[4] M. Audronis, A. Leyland, P.J. Kelly, A. Mathews, Composition and structure-property relationships of chromium-diboride/molybdenium-disulphide PVD nano-composite hard coatings deposited by pulsed magnetron sputtering, Applied Physics A 91/1 (2008) 77-86.

[5] K. Lukaszkowicz, J. Sondor, A. Kriz, M. Pancielejko, Structure, mechanical properties and corrosion resistance of nanocomposite coatings deposited by PVD technology onto the X6CrNiMoTi17-12-2 and X40CrMoV5-1 steel substrates, Journal of Materials Science 45/6 (2010) 1629-1637.

[6] F. Vaz, L. Rebouta, P. Goudeau, J. Pacaud, H. Garem, J.P. Riviere, A. Cavaleiro, E. Alves, Characterisation of $Ti_{1-x}Si_xN_y$ nanocomposite films, Surface and Coatings Technology 133-134 (2000) 307-313.

[7] A.A. Voevodin, J.S. Zabinski, Nanocomposite and nanostructured tribological materials for space applications, Composites Science and Technology 65/5 (2005) 741-748.

[8] S. Veprek, M.J.G. Veprek-Heijman, Industrial applications of superhard nanocomposite coatings, Surface and Coatings Technology 202/21 (2008) 5063-5073.

[9] Y.C. Cheng, T. Browne, B. Heckerman, E.I. Meletis, Mechanical and tribological properties of nanocomposite TiSiN coatings, Surface and Coatings Technology 204/14 (2010) 2123-2129.

[10] K. Polychronopoulou, M.A. Baker, C. Rebholz, J. Neidhardt, M. O`Sullivan, A.E. Reiter, K. Kanakis, A. Leyland, A. Matthews, C. Mitterer, The nanostructure, wear and corrosion performance of arc-evaporated CrB_xN_y nanocomposite coatings, Surface and Coatings Technology 204/3 (2009) 246-255.

[11] S. Zhang, N. Ali, Nanocomposite Thin Films and Coatings, Imperial College Press, London, 2007.

[12] D. Pakuła, L.A. Dobrzański, A. Kriz, M. Staszuk, Investigation of PVD coatings deposited on the Si_3N_4 and sialon tool ceramics, Archives of Materials Science and Engineering 46/1 (2010) 53-60.

[13] Ö. Altun, Y.E. Böke, Effect of the microstructure of EB-PVD thermal barrier coatings on the thermal conductivity and the methods to reduce the thermal conductivity, Archives of Materials Science and Engineering 40/1 (2009) 47-52.

[14] L.A. Dobrzański, L.W. Żukowska, J. Mikuła, K. Gołombek, T. Gawarecki, Hard gradient (Ti,Al,Si)N coatings deposited on composite tool materials, Archives of Materials Science and Engineering 36/2 (2009) 69-75.

[15] A.J. Novinrooz, A. Afshari, H. Seyedi, Improvement of hardness and corrosion resistance of SS-420 by Cr+TiN coatings, Journal of Achievement in Materials and Manufacturing Engineering 23/1 (2007) 43-46.